

Phononic crystals

J. H. Page^{* 1}, **Alexey Sukhovich**¹, **Suxia Yang**^{** 1, 2}, **M. L. Cowan**^{*** 1},
François Van Der Biest³, **Arnaud Tourin**³, **Mathias Fink**³, **Zhengyou Liu**⁴,
C. T. Chan², and **Ping Sheng**²

¹ Department of Physics and Astronomy, University of Manitoba, Winnipeg,
Manitoba R3T 2N2, Canada

² Department of Physics, Hong Kong University of Science and Technology, Kowloon,
Hong Kong, China

³ Laboratoire Ondes et Acoustique, ESPCI, Université Paris VII, UMR 7587, 10 rue Vauquelin,
75005 Paris, France

⁴ Department of Physics, Wuhan University, Wuhan 430072, China

Received 25 July 2004, revised 25 August 2004, accepted 15 October 2004

Published online 22 November 2004

PACS 43.35.+d, 63.20.–e

Phononic crystals are periodic composite materials with lattice spacings comparable to the acoustic wavelength. They are of interest not only because of the profound effects of their periodic structure on wave propagation (e.g., the existence of acoustic band gaps), but also because of potential applications (e.g., their possible role in sound filters, transducer design and acoustic mirrors). In this paper, we summarize recent progress using ultrasonic experiments to investigate both two- and three-dimensional phononic crystals. By measuring the ultrasonic wave field transmitted through slab-shaped samples of different thicknesses, both the dispersion curves and amplitude transmission coefficient can be determined. Because the field is pulsed, the dynamics of the wave fields can also be investigated; this has allowed us to make a systematic study of ultrasonic wave tunneling in phononic crystals. New results on resonant tunneling, focussing and negative refraction phenomena in phononic crystals are also presented. Our data are well explained using Multiple Scattering Theory, giving additional insight into the physical properties and potential applications of these novel materials.

© 2004 WILEY-VCH Verlag GmbH & Co. KGaA, Weinheim

1 Introduction

Phononic crystals are periodic composite materials, the constituents of which have different acoustic velocities and densities, with lattice constants on the scale of the wavelength of sound (or ultrasound) [1–14]. As such, they are the acoustic or elastic analogue of photonic crystals for light [15–22]. While some studies of periodic multilayered materials (1D phononic crystals) date back to the late 70s [23, 24], interest in phononic crystals, especially in two and three dimensions, has grown especially rapidly during the last decade [25]. Much of this recent activity is flourishing because phononic crystals provide some distinct advantages for studying the effects of lattice structure on the propagation of classical waves. For example, since both velocity and density differences contribute to the scattering contrast, phononic crystals with a wide range of scattering properties can be realized experimentally, and the existence of both longitudinal and transverse bulk waves, as well as surface waves, adds considerably to the richness of the underlying physics. Also, the development of powerful theoretical models and relative ease with which

* Corresponding author: e-mail: jhpage@cc.umanitoba.ca, Phone: +1 204 474 9852, Fax: +1 204 474 7622

** Current address: Department of Materials Science Engineering, University of Toronto, Toronto, Ontario M5S 3E4, Canada.

*** Current address: Department of Physics, University of Toronto, Toronto, Ontario M5S 3E4, Canada.

© 2004 WILEY-VCH Verlag GmbH & Co. KGaA, Weinheim

both amplitude and phase information can be extracted using pulsed ultrasonic and acoustic techniques, is really making it possible to study phononic crystal properties extensively. Much of the initial research focused on phononic band gaps, which occur due to Bragg scattering when the wavelength is comparable with the lattice constants, leading to frequency bands where wave propagation is forbidden. As a result, much is now known about the conditions under which phononic crystals with complete band gaps can be fabricated, allowing wave transport in this frequency range to be investigated and novel acoustic waveguides to be constructed [1–10]. Interesting ideas on how to construct compact phononic crystal sound insulators have also been proposed and demonstrated [5]. More recently, attention has turned to wave transport in the pass bands both below and above the band gaps, where unusual “negative refraction”, diffraction and focusing effects have been demonstrated [11–14].

In this paper, we summarize recent progress using a combination of experimental and theoretical methods to study ultrasonic wave transport in mostly three-dimensional (3D) phononic crystals [4, 8–10, 13]. These 3D crystals have been less studied experimentally than 2D structures [6, 7, 11, 12], reflecting the fact that 3D structures are more difficult to fabricate. We first describe the 3D crystals used in our experiments and summarize pulse propagation experiments that allow the transmission coefficient, the dispersion relation and the wave propagation dynamics to be investigated. In the band gap, we review the evidence for ultrasound tunnelling and examine its dynamics in the presence of absorption, which is always present to some degree in classical systems [9]. These experiments are compared with the predictions of Multiple Scattering Theory (MST), which is ideally suited to the spherical scattering geometry of our crystals. We further explore the analogy with the quantum tunnelling of a particle by presenting new data on the resonant tunnelling of ultrasound through double phononic crystals in both two and three dimensions. Above the first band gap, we then examine how phononic crystals can dramatically change the directions in which an incident wave travels, leading to the apparent negative refraction of sound at the interface. Direct evidence of this effect is shown by experiments using a two-dimensional prism constructed from a crystal of steel rods in water, and experiments and theory are described that demonstrate the use of negative refraction to focus ultrasound through a flat phononic crystal “lens” [13].

2 Experiment

The 3D crystals used in our experiments were made from monodisperse tungsten carbide beads surrounded by water [9]. The beads were 0.8 mm in diameter and were packed meticulously by hand, layer by layer, in close-packed face-centred cubic arrays, with the [111] direction perpendicular to the layers. This combination of solid spheres and liquid matrix has very high scattering contrast, with an impedance ratio of 60 for longitudinal waves, leading to the formation of a complete band gap for frequencies between 0.98 and 1.2 MHz [9]. To gain complementary information, 2D crystals were also assembled from steel rods immersed in water; two systems were studied: square arrays with a solid volume fraction $\phi = 0.22$ and triangular arrays with $\phi = 0.58$.

Ultrasonic pulse propagation through the crystals was measured by placing the crystals in a large water tank in between two immersion transducers, which acted as generator and detector [8–10]. The 3D crystals had to be supported on a substrate, which was made sufficiently thick that ultrasonic reflections in the substrate could be separated temporally and removed from the subsequent analysis of the signal transmitted through the crystal. For the 2D crystals, there was no need for a substrate, and the reference pulses were taken through water without the crystal in place. The frequency dependence of the phase velocity, the group velocity and the transmission coefficient was then measured by comparing the transmitted pulses with reference pulses that had travelled once through the substrate alone. The transmission coefficient was determined from the ratio of the amplitudes of the fast Fourier transforms (FFTs) of the transmitted and input pulses, the phase velocity from the cumulative phase difference of the FFTs, and the group velocity from the pulse transit time of digitally filtered narrow band pulses [9, 10]. Measurements on negative refraction and focusing were performed using a miniature hydrophone to scan spatial distribution of the transmitted field.

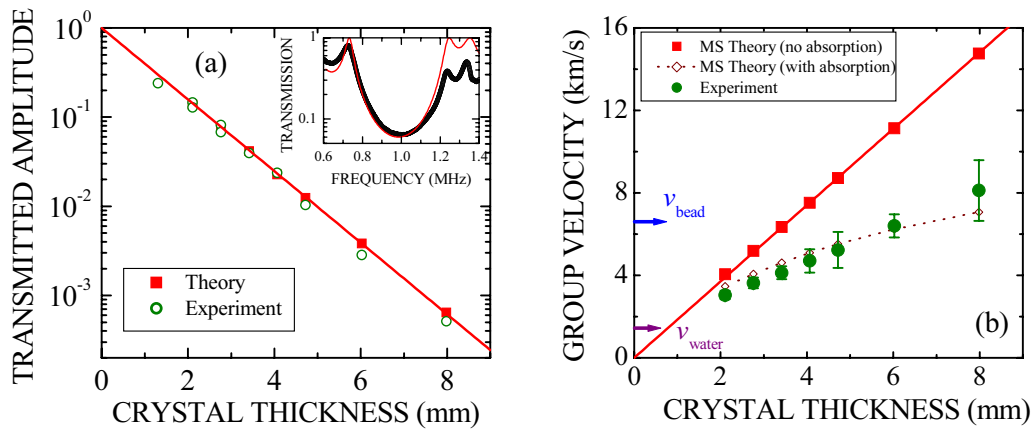


Fig. 1 (online color at: www.pss-b.com) (a) Thickness dependence of the amplitude transmission coefficient for fcc crystals of tungsten carbide beads in water. The insert shows the transmission as a function of frequency in the vicinity of the band gap for a four-layer crystal. (b) Comparison of theory and experiment for the thickness dependence of the group velocity.

3 Band gaps and tunnelling

To investigate the behaviour in the vicinity of the first band gap, the frequency dependence of the amplitude transmission coefficient T and group velocity v_g was measured for the 3D tungsten carbide phononic crystals [9, 10]. A broad dip in the transmission coefficient was found along the [111] direction near 1 MHz, as expected from the band structure calculated using Multiple Scattering Theory [4, 9], and the simple Bragg condition that half the wavelength be equal to the layer spacing. Typical results for a 4-layer thick sample are shown in the insert to Fig. 1(a). The thickness dependence of the transmission coefficient in the middle of the gap, at $f = 0.95$ MHz, is shown in the main part of this figure, indicating that $T(L)$ decreases exponentially with thickness L as $\exp(-\kappa L)$, consistent with evanescent modes having imaginary wave vector κ . This suggests that the ultrasonic pulse is transmitted through the crystal by tunnelling. To explore this phenomenon in more detail, we determined the group velocity by digitally filtering the transmitted and reference pulses with a narrow-band Gaussian bandpass filter centred on the frequency of interest, and measuring the peak delay time [9, 10]. Figure 1(b) shows that the group velocity increases linearly with sample thickness, an unusual result that is the classic signature of tunnelling, implying that the tunnelling time is independent of thickness. For the thickest crystals, the magnitude of v_g is remarkably fast – larger than any of the velocities of either constituent material. The solid and dashed curves in Fig. 1(b) are calculated using Multiple Scattering Theory both without and with absorption, which is introduced by making the moduli of the constituent materials complex. It can be seen that the theory with absorption gives a very satisfactory description of the experimental results, indicating how dissipation, which has no counterpart in the quantum tunnelling case, significantly affects the measured tunnelling time. This effect was interpreted using a so-called two modes model, which allows the role of absorption to be understood in simple physical terms [9, 10]. Absorption in the band gap of a phononic crystal cuts off the long multiple scattering paths, making the destructive interference that gives rise to the band gap incomplete. As a result, a small-amplitude propagating mode is produced in parallel with the dominant tunnelling mode, accounting for the reduction in the measured group velocity relative to the predictions without absorption. This simple model was also found to give a good quantitative explanation of the data [9, 10].

The demonstration that, in a band gap, ultrasound pulses travel through a phononic crystal by tunnelling raises an interesting question. Can the phenomenon of resonant tunnelling, analogous to the tunnelling of a quantum particle through a double barrier, be observed for phonons? This effect is intriguing since on resonance the transmission probability of a quantum particle through a double barrier is predicted to be unity, even though the transmission probability through a single barrier is exponentially

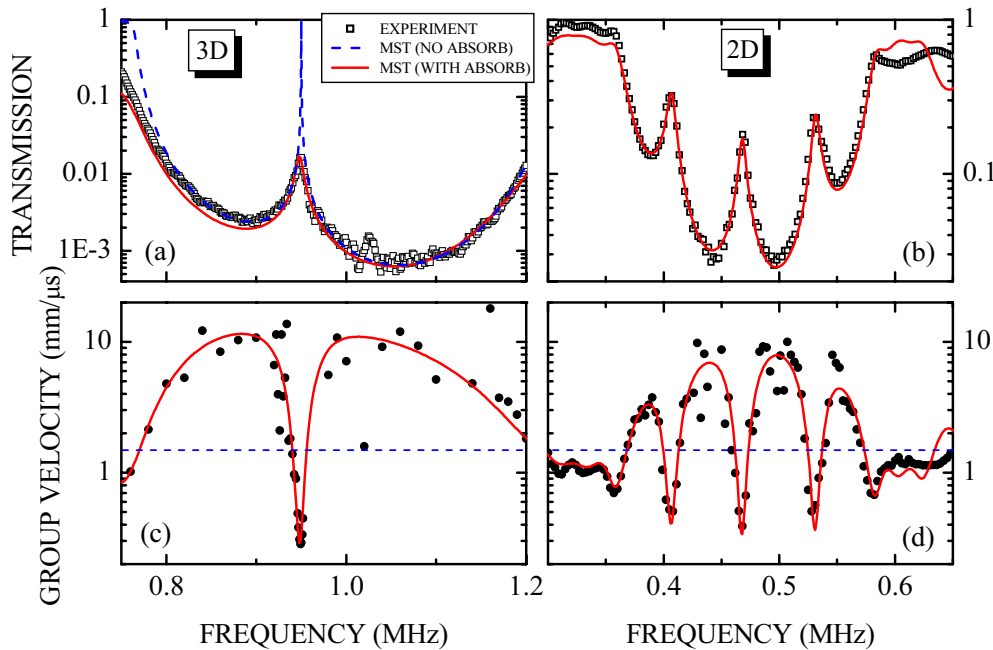


Fig. 2 (online color at: www.pss-b.com) (a) Amplitude transmission coefficient through a 3D double phononic crystal, with each crystal consisting of four layers of tungsten carbide beads in water. Data (symbols) are compared with the theoretical predictions of MST without (dashed line) and with (solid line) absorption in each phononic crystal. The absorption coefficient (imaginary wavevector) $\kappa_{\text{abs}} = 0.09 \text{ mm}^{-1}$. (b) Measured transmission through a 2D double four-layer crystal, compared with predictions of the 1D model ($\kappa_{\text{abs}} = 0.01 \text{ mm}^{-1}$). (c) and (d) Frequency dependence of the group velocity near resonance for the 3D and 2D double crystals, compared with MST and 1D theory respectively. The dashed horizontal line is the velocity in water.

small. Furthermore, the group time, which normally corresponds to the transit time of the particle, is predicted to grow exponentially with the thickness of a single barrier. To see if analogous effects occur in phononic crystals, we have made the phononic analogue of a double barrier by sandwiching a layer of uniform material between two phononic crystals, in both two and three dimensions. For the 3D resonant tunnelling experiment, a 7.05-mm-thick aluminium slab was placed between a pair of the tungsten carbide phononic crystals (i.e., the same 3D crystal system in which ultrasound tunnelling was demonstrated in [9]); these new experiments were performed for pairs of crystals, with their [111] directions perpendicular to the slab, consisting of two, three and four layers each. The aluminium thus formed a resonant cavity between the two crystals. The 2D crystals consisted of square arrays of steel rods in water (rod diameter = 0.8 mm, lattice constant = 1.5 mm), mounted in a supporting frame that allowed the crystals to be separated by an integer number of lattice constants.

Typical results for the frequency dependence of the transmission coefficient in the vicinity of the band gap are shown in Figs. 2(a) and (b) for the 3D and 2D crystals, respectively. In Fig. 2(a), a single resonant peak is seen in the middle of the gap, at a frequency that is within a few percent of the frequency at which the ultrasonic wavelength is equal to the thickness of the aluminum spacer. The slight difference in the resonant frequencies can be attributed to the phase shift acquired by the waves upon reflection from the interfaces between aluminium and each crystal. However, the magnitude of the experimental resonant peak is not unity, an effect that can be explained by absorption in the phononic crystals. This can be seen by comparing the solid and dashed curves in Fig. 2(a), which show the results of MST calculations with and without absorption: when no absorption is present, a peak magnitude of unity is indeed predicted, just as in the quantum case, but the peak is considerably reduced when absorption is included, in agreement with experiment. This effect can again be understood in simple physical terms by the two-modes model, since the small-amplitude propagating mode that is created in the band gap by

absorption increases the leakage from the cavity and lowers the quality factor Q of the resonance. Hence the resonant peak is broadened, and its maximum reduced. Similar behaviour is seen for resonant tunnelling in the 2D crystals (Fig. 2(b)), except that the resonant cavity is thicker in this case (equivalent to 6 missing rows of rods) and three distinct resonant tunnelling peaks are found in the gap. Since we are not yet able to calculate the transmission through the double crystal using MST, we have instead accounted for the essential physics using a simple 1D phononic crystal model, based on well established techniques for layered media [26]. Again the effect of absorption in each phononic can be included by making the wave vector complex, giving excellent agreement with the experimental results.

Since we use a pulsed technique, we can also investigate the dynamics of resonant tunnelling by measuring the group time and group velocity as a function of frequency. Results for the same two double crystals are shown in Figs. 2(c) and (d). While off resonance, very large velocities are found, characteristic of tunnelling, on resonance the wave pulses are dramatically slowed down, with velocities comparable to the speed of sound in air. Thus in sweeping through the resonance, the group velocity changes by approximately a factor of 50, encompassing both very fast and very slow sound. However, even though the measured group velocity is very slow on resonance, it is still larger than the velocity expected from the exponential increase in group time with thickness that is predicted in the absence of absorption. The physical basis for this difference can again be understood in terms of absorption, which affects the group velocity and group time in a similar way to the transmission peaks: because absorption introduces leakage into the cavity, the cavity dwell time of the pulse on resonance is reduced, and the velocity is not as slow. To calculate this effect quantitatively, we use the MST and the 1D model, with the same absorption coefficients that were used for the transmission calculations. The results are shown by the solid curves in Figs. 2(c) and (d), again giving very good agreement with experiment, and providing additional evidence of the large but also subtle effects of absorption on resonant tunnelling in acoustic systems.

4 Phonon focussing and negative refraction

Both below and above the band gap, wave propagation in phononic crystals is strongly influenced by crystalline anisotropy, leading to interesting effects arising from the fact that the group velocity, which represents the direction of energy transport by Bloch waves inside the crystal, is no longer parallel to the wave vector. In atomic crystals, analogous effects in phonon focussing have been extensively studied [27], but experiments are limited to the long wavelength regime where $\lambda \gg a$. To explore the higher frequency regime above the first band gap that is accessible in phononic crystals, we have investigated phonon focussing in the tungsten carbide/water phononic crystal by replacing the quasi plane-wave source used in the tunnelling experiments with a small-diameter ‘‘pinducer’’ (radius $\sim \lambda$) and imaging the transmitted field with a miniature hydrophone [13]. The experimental set-up is shown in Fig. 3(a). By scanning the hydrophone either parallel or perpendicular to the crystal surface on the far side of the substrate, and taking FFTs of the transmitted pulse at each hydrophone position, the transmitted field pattern at any frequency in the bandwidth of the pulse could be accurately measured.

Figure 3(b) shows the spatial variation of the detected field amplitude at $f = 1.57$ MHz, near the bottom of the third pass band. At this frequency, the diverging beam from the pinducer, which has a FWHM in the detection plane of 65 mm (more than three quarters of the width of the region imaged in the figure), is sharply focussed to a tight spot with a FWHM of only 5 mm. This example shows clearly that a phononic crystal with flat parallel planar faces can be used to focus ultrasound. One remarkable feature of these data is that such a sharp focal spot is observed in a plane quite far from the crystal; the distance from the crystal face to the detection plane is approximately 130 wavelengths, while the distance from the source to the crystal is only 2 wavelengths.

The origin of the focussing effect can be understood from the equifrequency (or slowness) surface, which represents the variation in the magnitude of the wave vector with direction at a given frequency. Figure 3(c) shows two cross sections of the equifrequency surfaces at 1.57 and 1.60 MHz, calculated in the reduced zone scheme using the MST [13]. Also shown by the dashed curve is the equifrequency surface for water, and a representative incident wave vector $\mathbf{k}_{\text{incident}}$ inclined away from the normal to the

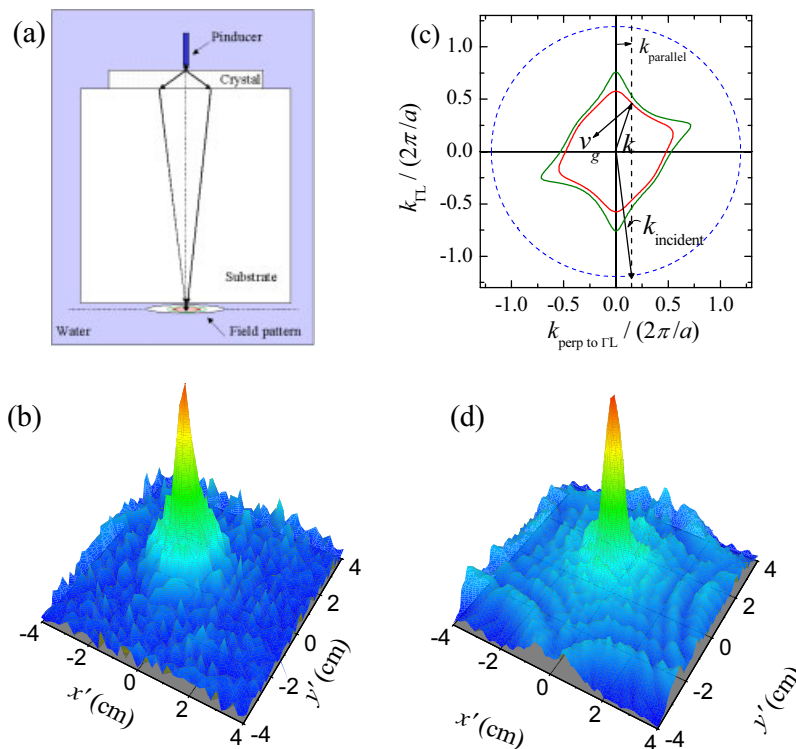


Fig. 3 (online color at: www.pss-b.com) (a) Schematic representation of the experimental setup for the phonon focussing experiments. The source is located 3 mm above the crystal, and the image is detected just below the substrate, approximately 130 wavelengths below the lower crystal surface. (b) Image of the source focussed by a 12-layer phononic crystal made from tungsten carbide beads. (c) Cross sections of the equifrequency surfaces of this phononic crystal at 1.57 (outer solid curve) and 1.6 MHz (inner solid curve) in a plane containing the [111], [110] and [001] directions. The dashed circle is the equifrequency contour for water. (d) Calculation of the field pattern using a Fourier imaging technique, based on the 3D equifrequency surfaces predicted by the MST.

surface of the crystal. The direction of the wave vector and group velocity for the corresponding Bloch waves inside the crystal are also shown for the inner phononic crystal equifrequency surface (1.6 MHz); these directions are determined by the boundary conditions that the component of the wave vector parallel to the surface ($k_{\text{par}} \perp k_{\text{TL}}$) must be equal both inside and outside the crystal (Snell's law) and the condition that v_g is normal to the equifrequency surface, since $v_g = \nabla_k \omega(k)$ [28]. Thus, for the waves to continue downwards towards the detector on the far side of the crystal, the group velocity must also point downwards, but its direction is substantially modified and points in a direction that corresponds to a negative angle of refraction. This occurs even though the wave vector obeys Snell's law in the usual way at each interface. It is this large negative refraction of Bloch waves inside the crystal, governed by the directions of the group velocity, that allows an image of the source to be formed on the far side of the crystal, as shown schematically by the "rays" drawn in Fig. 3(a).

To calculate the shape of the image quantitatively, we use a Fourier imaging technique, in which the input beam is Fourier transformed spatially into plane waves, and each plane wave is allowed to propagate through the crystal according to the wave vectors determined by the equifrequency surface. The boundary conditions at the front and back interfaces are correctly implemented according to Snell's law. The image in the detecting plane is then reconstructed by taking an inverse Fourier transform back into real space, giving the results shown in Fig. 3(d). Excellent agreement with experiment is seen, confirming that this model correctly incorporates the essential physics of this wave-focussing phenomenon.

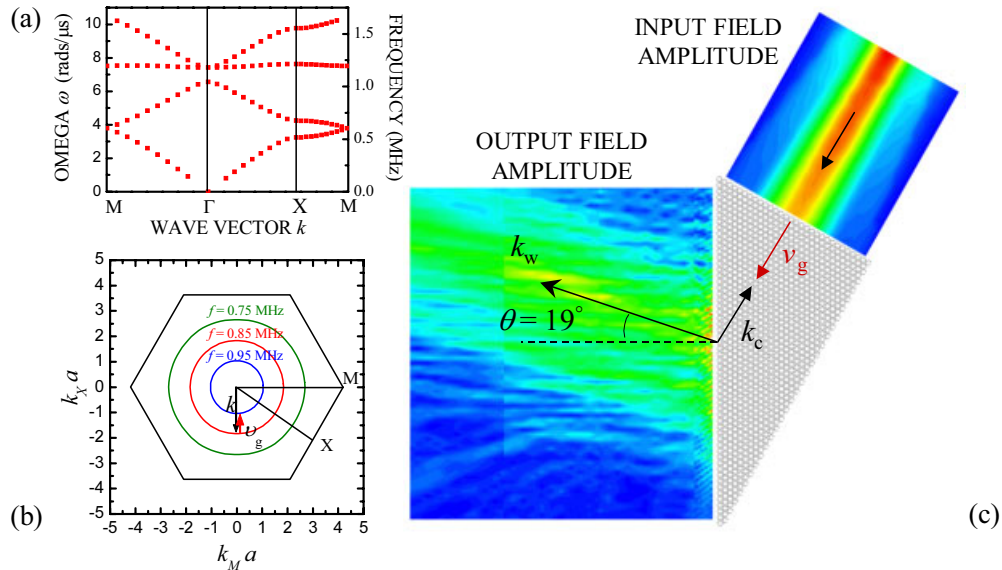


Fig. 4 (online color at: www.pss-b.com) (a) Band structure of a 2D hexagonal lattice of steel rods in water at a volume fraction of 58%, calculated by the MST. (b) Equifrequency contours and the first Brillouin zone at three frequencies in the second pass band. (c) Negative refraction in a 30° – 60° – 90° prism. The input field is incident from the upper right, and is refracted at a negative angle of 19° from the largest face of the prism.

To examine the phenomenon of negative refraction in phononic crystals more directly, we have constructed a 2D phononic crystal prism from steel rods, packed in a triangular lattice at a volume fraction of 58% and surrounded by water. The band structure for this crystal, calculated using the MST, is shown in Fig. 4(a). In the ΓX , or $[11]$, direction, there is a stop band around 0.6 MHz, and above the stop band there is a single branch, which appears quite isotropic. We have measured the transmission through a thin slab of this crystal, as well as the phase velocity, and have confirmed the location of the stop band and the shape of the dispersion curves in this direction. In the pass band above this stop band, we have also calculated the equifrequency contours, three of which are shown in Fig. 4(b). The contours are remarkably circular, indicating that in this frequency range, the reduced zone wave vector has the same magnitude in all directions. As a result, the wave vector points in the opposite direction to the group velocity, a situation that resembles the left-handed behaviour that has been discovered in negative index metamaterials [29]. This isotropic behaviour also indicates that this system would make an excellent superlens in this frequency range. Here we demonstrate the underlying negative refraction effect by measuring the incident and refracted waves from the right-angle prism shown in Fig. 4(c). A quasi-planar input beam is directed at normal incidence on the shortest face of the prism, which is perpendicular to the $[11]$ direction, and the field that emerges from the longest face is imaged using the miniature hydrophone. The resulting field pattern is also shown in Fig. 4(c), and is seen to bend backwards in the negative direction on leaving the crystal, showing that the dominant wave vector inside the crystal must point in the negative direction as predicted from the equifrequency contour. To emphasize this point, the directions of the Bloch wave vector and group velocity inside the crystal are also shown in Fig. 4(c), as well as the direction of the refracted beam outside. Furthermore, the measured refraction angle, 19° , is in excellent agreement with calculations based on the equifrequency contour at 0.85 MHz from the MST. At this frequency, the magnitude of the reduced zone wave vector inside the crystal is predicted to be 1.425 mm^{-1} , and the wave vector in water is 3.85 mm^{-1} , so that the application of Snell's law at the interface, $k_c \sin 60^\circ = k_w \sin \theta_w$, gives a refraction angle in water θ_w of 20.1° . Similar good agreement is found between the MST predictions and experiment at other frequencies in the band, giving additional evidence of negative refraction in phononic crystals.

5 Conclusions

Ultrasonic pulse propagation in phononic crystals is making an important contribution to understanding wave transport in ordered structures. Because the wave field is measured directly in ultrasonic experiments, a complete picture of wave propagation is accessible, allowing the transmission coefficient, the dispersion relations and the dynamics of the wave fields to be investigated. In this paper, we have reviewed recent progress in understanding two different types of wave phenomena in both 2D and 3D phononic crystals. The first of these is ultrasound tunnelling in the band gap of a single phononic crystal, and the related phenomenon of resonant tunnelling in double phononic crystals. The second is focussing of ultrasound in through a flat phononic crystal by negative refraction. The unusual effect of negative refraction was also investigated in experiments and theory for a 2D phononic crystal prism. Multiple Scattering Theory was found to give an excellent description of the experimental results, showing the power of this analytic approach to calculating and understanding the properties of phononic crystals with simple scattering geometries.

Acknowledgements Support from NSERC of Canada, the University of Manitoba Graduate Fellowship program, RGC (HKUST6143/00P) of Hong Kong, and NSFC (10174054) is gratefully acknowledged. We would also like to thank Maria Kafesaki and Costas Soukoulis for discussions of negative refraction.

References

- [1] E. N. Economou and M. M. Sigalas, *Phys. Rev. B* **48**, 13434 (1993); *J. Acoust. Soc. Am.* **95**, 1734 (1994).
- [2] M. S. Kushwaha, P. Halevi, L. Dobrzynski, and B. Djafari-Rouhani, *Phys. Rev. Lett.* **71**, 2022 (1993).
M. S. Kushwaha, B. Djafari-Rouhani, L. Dobrzynski, and J. O. Vasseur, *Eur. Phys. J. B* **3**, 155 (1998).
- [3] M. Kafesaki and E. N. Economou, *Phys. Rev. B* **60**, 11993 (1999).
I. E. Psarobas, N. Stefanou, and A. Modinos, *Phys. Rev. B* **62**, 278 (2000).
- [4] Z. Liu, C. T. Chan, P. Sheng, A. L. Goertzen, and J. H. Page, *Phys. Rev. B* **62**, 2446 (2000).
- [5] Z. Liu, X. Zhang, Y. Mao, Y. Y. Zhu, Z. Yang, C. T. Chan, and P. Sheng, *Science* **289**, 1734 (2000).
- [6] M. Torres, F. R. Montero de Espinosa, and J. L. Aragón, *Phys. Rev. Lett.* **86**, 4282 (2001).
- [7] J. O. Vasseur, P. A. Deymier, B. Chenni, B. Djafari-Rouhani, L. Dobrzynski, and D. Prevost, *Phys. Rev. Lett.* **86**, 3012 (2001).
- [8] J. H. Page, A. L. Goertzen, S. Yang, Z. Liu, C. T. Chan, and P. Sheng, in: *Photonic Crystals and Light Localization in the 21st Century*, edited by C. M. Soukoulis, NATO Science Series C, Vol. 563 (Kluwer, Dordrecht, 2002), p. 59.
- [9] S. Yang, J. H. Page, Z. Liu, M. L. Cowan, C. T. Chan, and P. Sheng, *Phys. Rev. Lett.* **88**, 104301 (2002).
- [10] J. H. Page, S. Yang, M. L. Cowan, Z. Liu, C. T. Chan, and P. Sheng, in: *Wave Scattering in Complex Media: From Theory to Applications*, edited by B. A. van Tiggelen and Sergey Skipetrov (Kluwer Academic Publishers: NATO Science Series, Amsterdam, 2003), p. 283.
- [11] F. Cervera, L. Sanchis, J. V. Sanchez-Perez, R. Martinez-Sala, C. Rubio, and F. Meseguer, *Phys. Rev. Lett.* **88**, 023902 (2002).
B. C. Gupta and Z. Ye, *Phys. Rev. E* **67**, 036603 (2003).
- [12] N. Garcia, M. Nieto-Vesperinas, E. V. Ponzovskaya, and M. Torres, *Phys. Rev. E* **67**, 046606 (2003).
- [13] S. Yang, J. H. Page, Z. Liu, M. L. Cowan, C. T. Chan, and P. Sheng, *Phys. Rev. Lett.* **93**, 024301 (2004).
- [14] X. Zhang and Z. Liu, *Appl. Phys. Lett.* **85**, 341 (2004).
- [15] E. Yablonovitch, *Phys. Rev. Lett.* **58**, 2059 (1987).
E. Yablonovitch and T. J. Gmitter, *Phys. Rev. Lett.* **63**, 1950 (1989).
- [16] S. John, *Phys. Rev. Lett.* **58**, 2486 (1987).
- [17] J. D. Joannopoulos, R. D. Meade, and J. N. Winn, *Photonic Crystals* (Princeton University Press, Princeton, 1995).
- [18] H. Kosaka, T. Kawashima, A. Tomita, M. Notomi, T. Tamamura, T. Sato, and S. Kawakami, *Phys. Rev. B* **58**, 10096 (1998); *Appl. Phys. Lett.* **74**, 1212 (1999); *Appl. Phys. Lett.* **74**, 1370 (1999).
- [19] M. Notomi, *Phys. Rev. B* **62**, 10696 (2000).
J. Mizuguchi, Y. Tanaka, S. Tamura, and M. Notomi, *Phys. Rev. B* **67**, 075109 (2003).
- [20] S. Foteinopoulou, E. N. Economou, and C. M. Soukoulis, *Phys. Rev. Lett.* **90**, 107402 (2003).
E. Cubukcu, K. Aydin, E. Ozbay, S. Foteinopoulou, and C. M. Soukoulis, *Science* **423**, 604 (2003).
- [21] P. V. Parimi, W. T. Lu, P. Vodo, and S. Sridhar, *Nature* **426**, 404 (2003).

- [22] C. Luo, S. G. Johnson, J. D. Joannopoulos, and J. B. Pendry, *Phys. Rev. B* **68**, 045115 (2003).
- [23] V. Narayanamurti, H. Stormer, M. A. Chin, A. C. Gossard, and W. Wiegmann, *Phys. Rev. Lett.* **43**, 2012 (1979).
- [24] For more recent work on superlattices, see, e.g. S. Tamara, and J. P. Wolfe, *Phys. Rev. B* **36**, 3491 (1987); *Phys. Rev. B* **38**, 5610 (1998).
S. Mizuno and S. Tamara, *Phys. Rev. B* **50**, 7708 (1994).
M. Narita, Y. Tanaka, and S. Tamara, *J. Phys.: Condens. Matter* **14**, 1709 (2002).
- [25] For a comprehensive list of references on phononic crystals, see the Phononic Crystal database at www.phys.uoa.gr/phononics/PhononicDatabase.html.
- [26] L. Brekhovskikh, *Waves in layered media* (Academic Press, New York, 1960).
- [27] J. P. Wolfe, *Imaging Phonons: Acoustic Wave Propagation in Solids* (Cambridge University Press, Cambridge, 1998).
- [28] Note that Snell's law is not modified by a reciprocal lattice vector \mathbf{G} of the phononic crystal in these experiments, since the smallest G in the plane of the interface is larger than k_{incident} .
- [29] J. B. Pendry, *Phys. Rev. Lett.* **85**, 3966 (2000).